

Solid-state 94 GHz Doppler radar for meteorology

Dirk Klugmann¹ and Hui Wang²

STFC / Rutherford Appleton Laboratory, Harwell Campus, Didcot, Oxfordshire, OX11 0QX

¹*dirk.klugmann@stfc.ac.uk*

²*hui.wang@stfc.ac.uk*

Keywords: Millimetre wave radar, cloud radar, solid state components, atmospheric observations, meteorology

Abstract

Cloud radars based on solid-state component technology provide an efficient system architecture with attributes of relatively small size, low mass and low power consumption. These benefits are important and allow a wider application of cloud radar systems for meteorological sounding, easier deployment at remote locations, and reduced manufacturing costs.

More than a decade ago the Rutherford Appleton Laboratory began development of a frequency modulated continuous wave (FMCW) cloud radar profiler based on solid-state components. Several systems have been produced and applied for atmospheric observations and research. Recent technical development and increased requirements of the scientific community have encouraged the development of an upgraded radar incorporating a Doppler sounding capability. This paper describes the proposed methodology of this technical enhancement.

After the description of the principle of FMCW Doppler radar, the current design is explained and the upgraded design is introduced. The latter aims to provide

- Introduction of Doppler capability
- Simplification of design where appropriate
- Maximum utilisation of in-house capabilities

For achieving the last bullet point, a number of components or sub-systems have been included into the design. These are described in further detail.

Results achieved from the development activities to date are reported, which include a direct digital synthesiser (DDS) proposed to be utilised in the design and components or sub-systems based on in-house capabilities. The final section of this publication provides the conclusion and outlook.

1. Introduction

Millimetre-wave radar has been successfully applied in atmospheric research for a number of decades. First applications at K_a-band by NOAA ETL (1), (2) and at W-band by Miami University (3) were based on vacuum tube technology and used the pulsed Doppler operation mode. Due to the high manufacturing costs and high operation costs, these systems were exclusively used for atmospheric research, typically in time-restricted research campaigns. There was no

reasonable path foreseen to routine operational application, e.g. in networks of national weather services.

In the mid-1990s the first millimetre-wave radar profiler for atmospheric research based on solid-state devices (4) was developed in collaboration between University of Hamburg and Technical University Hamburg-Harburg. This system operated at W-band and used the Frequency Modulated Continuous Wave (FMCW) Doppler operation mode, which is much better suited for power generation by solid-state components than the pulsed operation mode. Around the same time the Rutherford Appleton Laboratory developed a millimetre-wave radar profiler based on semiconductor devices that operated in non-Doppler FMCW mode (5), (6). This system originally operated at V-band but later was converted to operation in W-band (7). These systems provided the first hint of operational capabilities that might make millimetre wave radars suitable for the operational networks of national weather services and similar organisations.

The original W-band radar cloud profiler developed by the Rutherford Appleton Laboratory was deployed and operated by the UK Meteorological Office at various sites for applications in atmospheric research and atmospheric observations. The Rutherford Appleton Laboratory manufactured further two similar W-band radar cloud profiler. One was delivered to the University of Marburg, Germany, the second was retained for in-house applications in the Earth Observation and Atmospheric Science Division. Results from atmospheric research since the development of the original system and recently increased demands on the capability of radars for cloud research have identified the requirement to improve the existing radar design, specifically by adding Doppler capability. It is also desirable to make use of the in-house capabilities in millimetre-wave technologies, which have advanced considerably since the original design was developed, in this process.

The approach to this improvement is described in the following sections. Some examples of the current progress are also provided.

2. Methodology

The improved design was developed based on the technology and the components applied in the original design. From this starting point the design was simplified where possible, and previously utilised components were replaced by components based on in-house capabilities (bonding, packaging, and manufacturing of components or sub-systems).

2.1. Principle of FMCW Doppler radar

The basic principle of FMCW Doppler operation, as e.g. described in (8), is visualised in Figure 1. The specific values given in this example are typical for FMCW Doppler radar operated at cm wavelengths, but the principle is the same for millimetre wave cloud radar. A series of frequency chirps with a modulation bandwidth B and a repetition rate f_{SREPW} are transmitted into the atmosphere. The frequency modulation function is depicted by the green line. The frequency modulation function for a signal scattered back from a single target at 30 km distance is given by the red line. This lags behind the frequency modulation function of the transmitted wave due to the travel time of the wave to the scattering target and back to the radar.

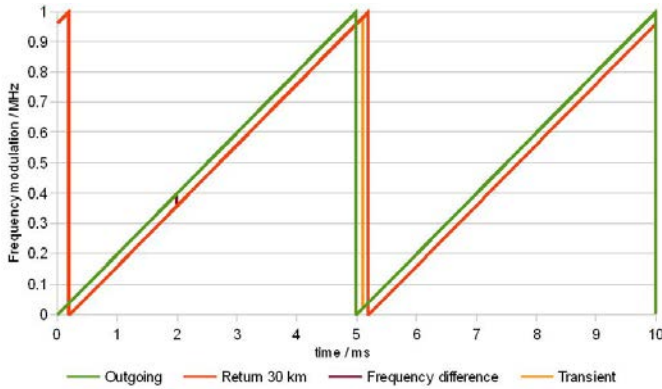


Figure 1: Principle of FMCW radar.

Consequently there is a fixed frequency difference between the transmitted and the backscattered wave for most of the duration of the frequency chirp, indicated by the short brown vertical line at $t = 2$ ms. For atmospheric targets, any Doppler shift during this period is typically negligible. At the end of the frequency chirp, when the frequency of the transmitted wave has been reset to the carrier frequency and started to ramp up again, there is a (typically short) period when the frequency difference between the transmitted and the received signal is much higher. This is indicated by the long yellow vertical line at $t = 5.1$ ms.

Though the Doppler shift for atmospheric targets is typically negligible during the period of a single frequency chirp, it can be observed by evaluating the signal recorded during a number of consecutive frequency chirps. The phase shift of the backscattered wave caused by a target moving lateral to the radar waves from one frequency chirp to the next causes a measurable frequency offset.

Typically a cloud radar will not receive a backscattered signal from a single target, but from thousands or even millions of targets per m^3 . Thus the return from the atmosphere for an FMCW Doppler radar is classified by range, and within each range by power within the radial velocity bins assigned to each range. For well-calibrated radar profilers this enables derivation of profiles of droplet (in cloud) or drop (in drizzle / rain) size distributions.

Interpreting the returned signal is a complex process involving the generation and addition of a sequence of returned signal power spectra. The process starts with recording the signal of the radar return from the atmosphere – backscattered from myriad atmospheric scatterers – over a number of consecutive frequency chirps. This recorded signal is Fourier transformed – typically by applying a Fast Fourier

Transform (FFT) algorithm – and a power spectrum is generated from it. Usually a number of consecutively generated power spectra are averaged with the purpose of reducing the variability of the spectral noise and increasing the detection sensitivity. A typical averaging time used for radar cloud profilers is 1 s.

Following the principle sketched above, there are some basic relationships in evaluating the atmospheric return spectrum from an FMCW Doppler radar. For instance, the range resolution is given by $\Delta R = c/2B$, where c indicates the speed of light. Consequently the range of an individual target occurring in the spectrum at frequency f_t can be assessed by the relationship $R = m \cdot \Delta R (\pm \Delta R/2)$, where $m \in \mathbb{N}$ is given by the equation $m = \text{round}(f_t/f_{\text{SW}})$. The unambiguously covered velocity range is $\Delta v = v_{\text{max}} - v_{\text{min}} = \frac{c}{2} \cdot \frac{f_{\text{SW}}}{f_0}$. The velocity of a target relative to the radar occurring at frequency f_t in the power spectrum can be calculated applying the relation $v_t = \frac{c}{2f_c} \cdot \Delta f (\pm \frac{c}{2f_c} \cdot \sigma f)$ where $\Delta f = f_t - m \cdot f_{\text{SW}}$, the carrier frequency of the radar is denoted by f_c , and σf is the spectral resolution of the power spectrum. The frequency shift Δf originates from the chirp-to-chirp changes in the phase of the electromagnetic waves scattered at the individual target. The power spectrum obtained by an FMCW Doppler radar consist of the sum of all spectra scattered by any individual target in the radar's observing volume.

2.2. Existing non-Doppler Radar design

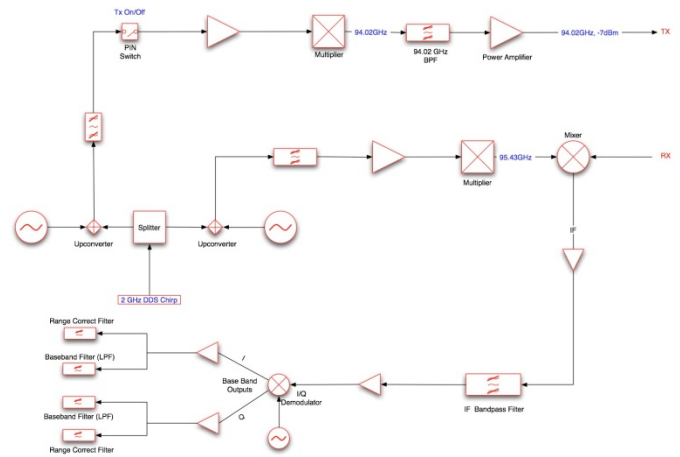


Figure 2: RF design of the existing radar cloud profiler.

The existing W-band radar cloud profiler is based on a heterodyne RF design as displayed in Figure 2. The primary source signal for the transmitting branch and the primary reference signal for the receiving branch are provided by two highly stable oscillators operating at slightly offset frequencies. A common chirp generated by a Direct Digital Synthesiser (DDS) is added to each signal. Both branches incorporate frequency multiplication by the same factor as well as a number of passive and active components. In the receiving branch the resultant signal is used as the local oscillator (LO) for the initial down-converter processing the waves scattered from atmospheric targets. The frequency offset between the transmitting and the receiving branch defines the IF after this initial down-converter. This is eventually compensated by a third highly stable oscillator operated at the same multiple of the frequency difference between the principal oscillators as applied in the frequency multipliers. This provides the LO for the final I/Q demodulation of the IF signal into base band.

The detailed design and optimization methodology (11) (12) combines three-dimensional electromagnetic modelling using HFSS (Ansys) with harmonic balance simulation using ADS (Keysight). The predicted performance of the frequency tripler is presented in Figure 5. The fundamental to third harmonic power conversion efficiency was optimized for an input power of 100 mW and fixed bias voltage of -7.46 V. The maximum calculated efficiency was around 15%, with a 3dB bandwidth from 79 to 103 GHz.

2.4.2. W-band third harmonic down-converter

A second area of component development relates to the harmonic down-converter. In this case, our approach is to simplify the mixer LO provision by using a third harmonic mixer configuration. The conversion loss of such a device is higher than for a conventional fundamental or subharmonic mixer, but simulations suggest that its performance will be adequate for use in the radar. With the availability of low noise amplifiers at the W-band frequency range, the harmonic down-converter can be used as the second stage in the receiver.

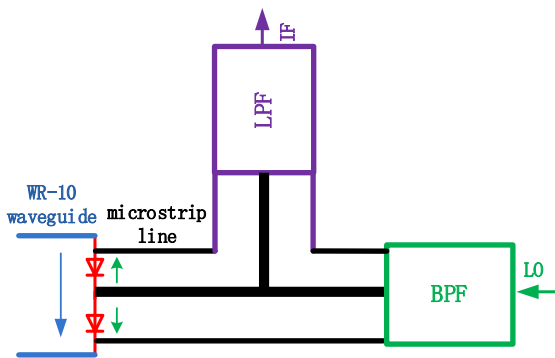


Figure 6: Schematic of third harmonic Schottky diode mixers.

RAL has developed a third harmonic mixer, based on a discrete Schottky diode. The mixer schematic is shown in Figure 6; it is a cross-bar balanced configuration utilizing a pair of diodes which are physically located in the RF waveguide. The matching circuit is on quartz substrate microstrip line, the block is split in the E-plane of the RF waveguide and the LO signal is introduced via a coaxial SMA connector. A LPF and a coupled-line Band pass filter (BPF) are used to separate the IF and LO signal.

The performance of the mixer is predicted by using the harmonic balance code. The LO power coupling for this mixer was optimized at 31.8 GHz, and this mixer requires 2 mW of LO power to achieve a minimum mixer conversion gain at a given frequency. The expected mixer DSB conversion loss is approximately 10 dB.

2.4.3. W-band amplifiers

Two types of W-band amplifier have been packaged successfully in-house and will be applied for the demonstrator laid out in Figure 3. Both incorporate the NG APH631 MMIC amplifier chip and a DC bias circuit. The moderate power version only incorporates one of these MMIC amplifier chips, while the higher power version applies power combining of two MMIC amplifier chips.

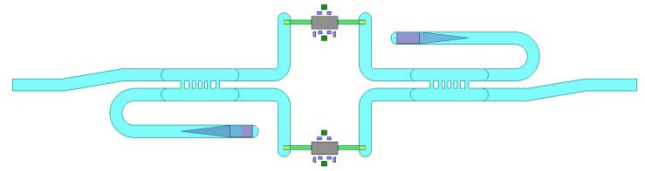


Figure 7: Schematic of the WR10 waveguide hybrids used as the power splitter and combiner.

In W-band, there are two commonly used circuits to realize power splitting/combining; the waveguide Y-junction coupler and quadrature hybrids. Due to its simplicity, the Y-junction coupler provides poor isolation between the two output ports. This disadvantage may deteriorate output return loss and cause potential instability for amplifiers. Thus waveguide quadrature hybrids are used for the power splitting and combining in the in-house design. A waveguide hybrid is a four-port directional coupler. It consists of two parallel waveguides coupled through a series of branches. Ideally, the power input on any port is equally divided by the two output ports with a phase difference of 90°. The schematic of this is displayed in Figure 7. A photograph showing the internal view of the manufactured higher power amplifier is presented in Figure 8.

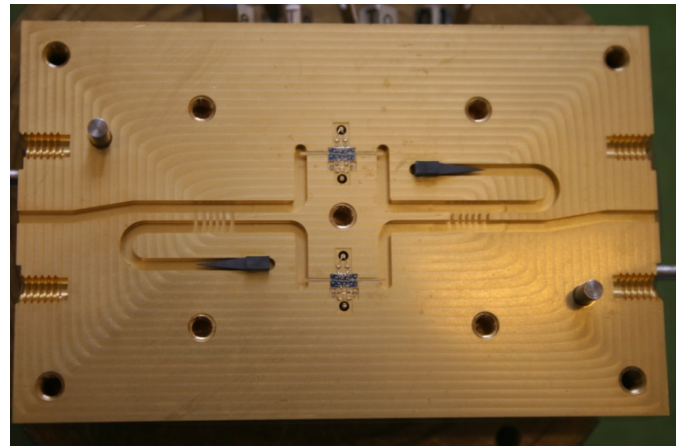


Figure 8: Internal view of the higher power amplifier utilising waveguide hybrids as power splitter and combiner.

3. Results

This section reports initial results from the components that already have been set up and assessed in the process of realising the Doppler capable simple demonstrator RF design visualised in Figure 3.

3.1. Primary signal generation by DDS

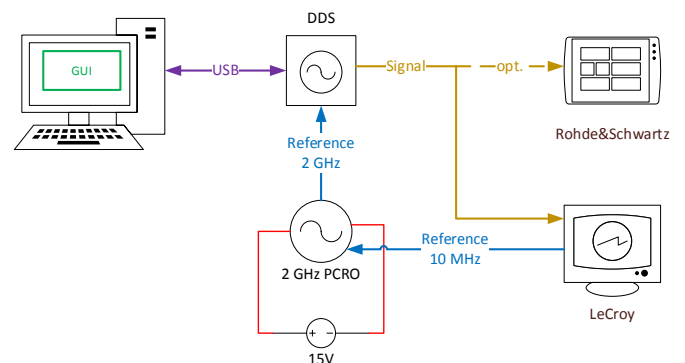


Figure 9: Basic test setup for the DDS.

The basic test set-up for the applied DDS is displayed in Figure 9. The DDS was supplied with a 2 GHz reference signal from a PCRO, which in turn was supplied with a 10 MHz reference signal from the LeCroy 6104 oscilloscope with spectrum analyser capability used for the assessment of the DDS. The DDS was controlled via USB connection from a PC alternatively by the GUI provided by the DDS manufacturer or by LabVIEW code. The latter closely follows an example provided by the manufacturer and is displayed in Figure 10.

The resulting frequency spectrum from a 5 MHz chirp on top of a carrier frequency of 750 MHz is shown in Figure 11. The reference power level (at the top of the graph) is -30 dBm. The vertical resolution is 10dB/Div, the centre frequency is 750 MHz, and the bandwidth is 100 MHz. The spectral resolution was 406.2 Hz, and 256 spectra were averaged.

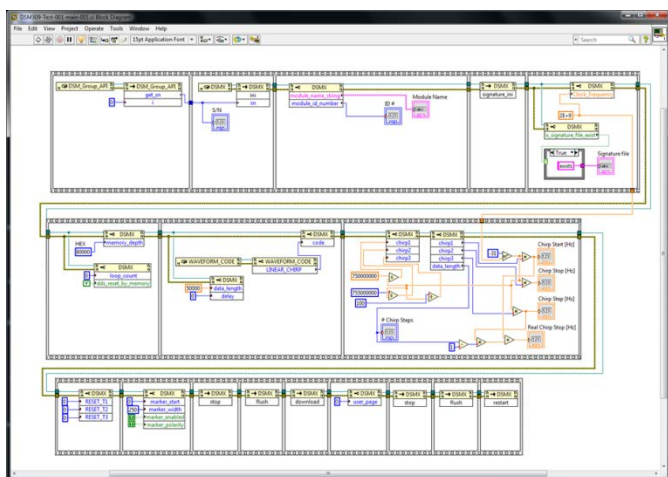


Figure 10: Sample LabVIEW VI for controlling the DDS.

The graph in Figure 11 displays some spurious frequency lines starting 25 MHz above and 30 MHz below the desired chirp frequency band. These, however, are in the worst case 50 dB below the spectral in-band power, which added up to a total power in the chirp band of approx. 5 dBm (non-calibrated measurement). It also should be mentioned that the power level at either end of the graph corresponds to the internal power level of the oscilloscope as recorded without input signal.

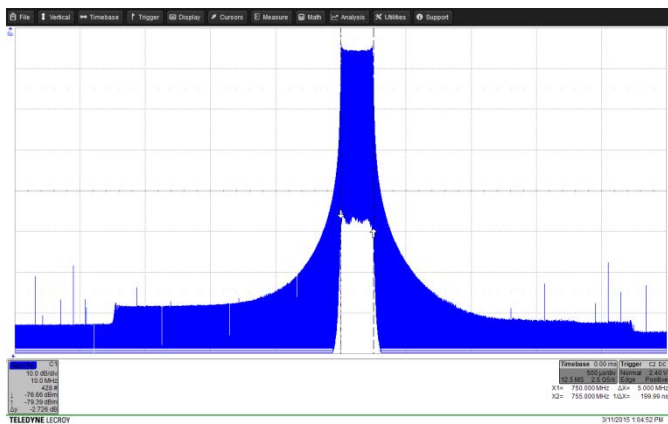


Figure 11: Spectrum of a 5 MHz chirp on top of a carrier frequency of 750 MHz.

3.2. W-band Schottky diode frequency tripler

The frequency tripler was tested using a signal source generator from Hittite, model HMC-T2270, and calibrated

Agilent power sensor. The maximum power available from the source varied from 100 to 60 mW over the frequency range 22.5 - 37 GHz. The measured results are presented in Figure 12, where the DC bias was optimized at each frequency. In this figure the full curve with open circle marks presents the measured conversion efficiency with respective input and output power levels shown by the dotted line with filled circles and dashed curve with points.

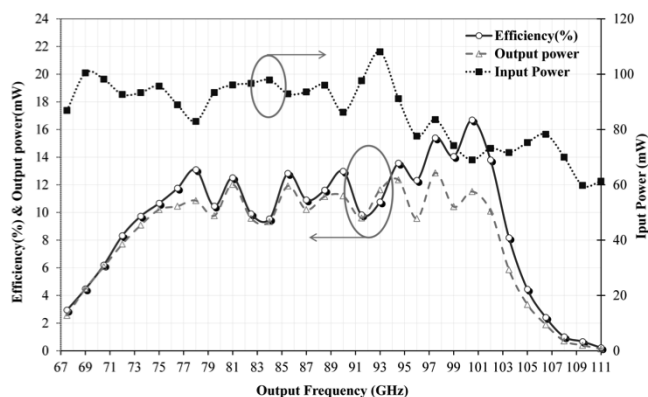


Figure 12: Measurement results of the W-band frequency tripler.

The peak power conversion efficiency was 16.7 % and the efficiency was above 5% over the range 69.5-105 GHz and 10% over the range 73-103 GHz. There is good agreement between the predicted and measured maximum efficiencies, although optimum performance is shifted upwards from 93 to 101 GHz.

The spectral purity of the multiplier's output signal was verified using a Rohde and Schwarz FSU26 spectrum analyser with external harmonic mixers. The fourth harmonic signal was found to be at least 30 dB below the third harmonic signal.

3.3. W-band third harmonic down-converter

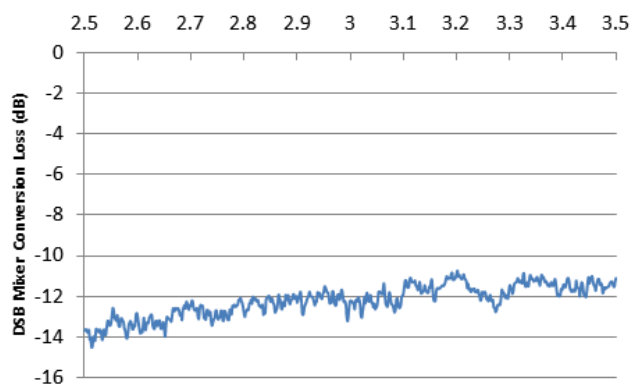


Figure 13: Preliminary measurement results of the W-band third harmonic mixer: DSB mixer conversion loss versus IF.

The classical Y-factor technique was used to test the system using ambient and liquid nitrogen-cooled loads as blackbody references. The equivalent noise temperature of the receiver was measured by presenting alternatively a room temperature and a liquid nitrogen-cooled blackbody in front of the mixer feed-horn, then calibrating the noise temperature of the IF chain. Figure 13 shows the preliminary mixer conversion loss from 2.5-3.5GHz. The measurement was done at fixed LO frequency of 31.8GHz. A band pass filter (BPF) has been used before the LO input. Further characterization is required

to finalize the mixer towards deployment in a radar system.

3.4. W-band amplifiers

The amplifier modules were tested using Agilent's vector network analyser (VNA) N5225A with Virginia Diodes Inc. (VDI) WR10 waveguide extenders. The parameters measured were:

- The gain (only for the single chip amplifier, see Figure 14)
- The saturation output power
- Return loss at both input and output ports

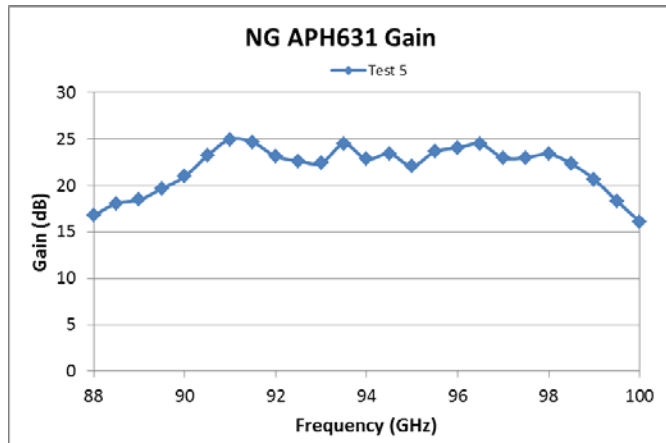


Figure 14: Gain of the single chip moderate power amplifier.

An attenuator inserted between the amplifier modules and the receiver extender ensured the output power of the modules was not exceeding the receiver's handling limit. Both the insertion loss of the attenuator and the input power level into the amplifier module were calibrated.

In the higher power amplifier employing power combining of two MMIC amplifier chips, the two chips were biased separately. By tuning the gate and drain voltages, optimum output power was achieved when the drain current was 230mA with the input power set to 6-7dBm.

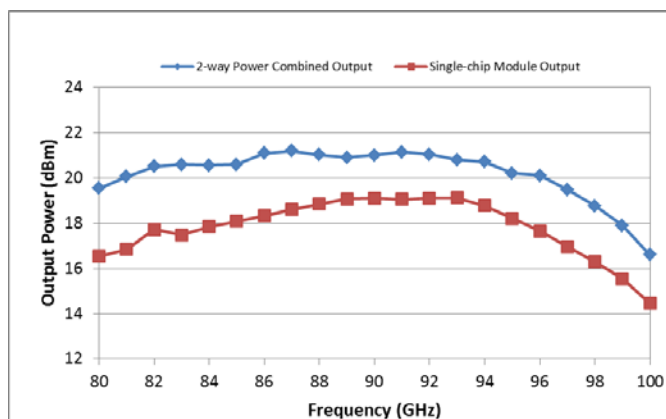


Figure 15: Comparison of the saturated output power between the single-chip amplifier and the 2-way power combined amplifier.

Figure 15 shows that the higher power amplifier achieves the expected higher saturated output power. It typically provides an output power that is between 2 and 3 dB higher than the single chip moderate power amplifier; a factor of less than

3dB is due to losses incurred by the in-waveguide power combining as e.g. described by (13).

4. Conclusion and outlook

Radar cloud profilers have been successfully applied in atmospheric research and climate monitoring. However, the wider utilisation of this class of instruments so far has been prevented by high costs of purchase and operation as well as technology which is not suitable for operational applications. Cloud radar systems based on solid state components could overcome this issue. The FMCW (Doppler) mode is more suitable for operating these devices than the pulsed mode due to the moderate peak power of solid-state components compared to vacuum tube based systems.

The Rutherford Appleton Laboratory has developed a radar cloud profiler based on solid state components. The system applies the FMCW operation mode, but is not Doppler capable. Three of these devices have been built and were successfully applied for atmospheric observations and research. However, recent technical progress and increased requirements of the atmospheric observations, atmospheric research and climate monitoring communities suggest the development of an improved design. This has been drafted with the aim to:

- Introduce Doppler capability
- Simplify the existing design where appropriate
- Maximise utilisation of in-house capabilities

The latter is achieved by incorporating as many components based on in-house development or production capabilities as possible. To date these are a W-band Schottky diode frequency tripler, a W-band third harmonic down-converter and W-band amplifiers.

Test results of the components based on in-house capabilities as well as of a DDS proposed for use in the design were presented. The next development steps will be the set-up of a simple demonstrator in UHF or L-band for testing the basic signal generation and the Data Acquisition / Digital Signal Processing system. This then will be extended to the simple Doppler capable demonstrator described in this publication. Eventually the final development state of the FMCW Doppler radar cloud profiler will be assembled and made available to the atmospheric observations, atmospheric research and climate monitoring communities.

5. Acknowledgement

The authors would like to thank Teratech Components for supplying the GaAs Schottky diodes used in this work. This work was partially supported by the UK's Science and Technology Facilities Council under the Proof of Concept contract POCF121302.

The authors further would like to thank Zhe Chen and Simon Rea for providing information, measurements and graphics on the in-house packaged amplifiers.

The authors also would like to thank Brian Ellison, Brian Moyna and Simon Rea for their helpful comments.

References

1. *A Millimeter-Wavelength Dual-Polarization Doppler Radar for Cloud and Precipitation Studies*. **Pasqualucci, F., et al.** 5, s.l. : American Meteorological Society, 1983, Journal of Applied Meteorology and Climatology, Vol. 22. ISSN: 0733-3021.
2. *The upgraded WPL dual-polarization 8-mm wavelength Doppler radar for micropysical and climate reserarch*. **Kropfli, R. A., Bartram, B. W. and Matrosov, S. Y.** San Francisco : American Meteorological Society, 1990. Proceeding Conference on Cloud Physics.
3. *Small Cumuli Observed with a 3-mm Wavelength Doppler Radar*. **Lhermitte, R. E.** 7, s.l. : American Geophysical Union, 1987, Geophysical Research Letters, Vol. 14. ISSN: 0094-8276 .
4. *A 94 GHz FM-CW Doppler Radar Profiler Using a Solid State Transmitter*. **Klugmann, D. and Judaschke, R.** 1, February 1996, Beitr. Phys. Atmosph, Vol. 69, pp. 239-246. ISSN: 0005-8173/96/01.
5. *Millimetre wave cloud radar*. **Ellison, B. N., Oldfield, M. and Bradford, W. J.** Toulouse : s.n., 2000. 9th International Workshop on the technical and scientific aspects of MST radar – MST9.
6. *Observing fog and low cloud with a combination of 78 GHz cloud radar and laser ceilometer*. **Lyth, D., Nash, J. and Oldfield, M.** Bucharest : WMO, 2005. WMO Tech. Conf. Meteorological & Environ. Inst Methods of Observation. p. P2(11).
7. *94 GHz FMCW Cloud Radar*. **Huggard, P. G., et al.** Cardiff : SPIE, 2008. SPIE Symposium 7117-3 on Millimetre Wave and Terahertz Sensors and Technology.
8. **Strauch, R. G.** *Theory and Application of the FM-CW Doppler Radar*. Electrical Engineering, Faculty of the Graduate School. Boulder, Colorado : University of Colorado, 1976.
9. *Novel 1-D microstrip PBG cells*. **Q. Xue, K.M. Shum and C.H. Chan.** 10, s.l. : IEEE Microw. Guided Wave Lett., 2000, Vol. 10.
10. *A Novel Compact Suspended Double Side CMRC Millimeter Bandpass Filter with Wide Stopband*. **X.F.Yang, Y. Fan, B. Zhang and M. Zhao.** s.l. : Progress In Electromagnetics Research Letters, 2011, Vol. 21.
11. **Wang, H.** *Conception et modélisation de circuits monolithiques à diode Schottky sur substrat GaAs aux longueurs d'onde millimétriques et submillimétriques pour des récepteurs hétérodynes multi-pixels embarqué sur satellites et dédiés à l'aéronomie ou la planétologi.* Universite Pierre et Marie Curie, Paris, France : Ph.D dissertation, 2009.
12. *A 540-640 GHz High Efficiency Four Anode Frequency Tripler*. **A. Maestrini, J. S. Ward, J. J. Gill, H. S. Javadi, E. Schlecht, C. Tripon-Canseliet, G. Chattopadhyay, and I. Mehdi.** s.l. : IEEE Transactions On Microwave Theory And Techniques, 2005, Vol. 53.
13. *Millimeter-Wave Power-Combining Techniques*. **Chang, Kai and Sun, Cheng.** 2, s.l. : IEEE, February 1983, IEEE Transactions on Microwave Theory and Techniques, Vols. MTT-31, pp. 91-107. ISSN: 0018-9480.